

Synthesis and Characterizations of Calcium Hydroxyapatite Derived from Crabs Shells (*Portunus pelagicus*) and Its Potency in Safeguard against to Dental Demineralizations *by*

FILE CRABB_INDAH.PDF (3.56M)

TIME SUBMITTED 17-JUL-2019 01:33PM (UTC+0700)

SUBMISSION ID 1152581449

WORD COUNT 4843

CHARACTER COUNT 24733

Research Article

1 Synthesis and Characterizations of Calcium Hydroxyapatite Derived from Crabs Shells (*Portunus pelagicus*) and Its Potency in Safeguard against to Dental Demineralizations

Indah Raya,¹ Erna Mayasari,¹ Afdaliah Yahya,¹
Muhammad Syahrul,¹ and Andi Ilham Latunra²

¹Chemistry Department, Faculty of Mathematics and Natural Sciences, Hasanuddin University, Makassar 90245, Indonesia

²Biology Department, Faculty of Mathematics and Natural Sciences, Hasanuddin University, Makassar 90245, Indonesia

Correspondence should be addressed to Indah Raya; indahraya05@gmail.com

Received 22 September 2014; Revised 31 January 2015; Accepted 23 February 2015

Academic Editor: Sean Peel

Copyright © 2015 Indah Raya et al. This is an open access article distributed under the Creative Commons Attribution License, which permits unrestricted use, distribution, and reproduction in any medium, provided the original work is properly cited.

Crab's shells of *Portunus pelagicus* species were used as raw materials for synthesis of hydroxyapatite were used for protection against demineralization of teeth. Calcination was conducted to crab's shells of *Portunus pelagicus* at temperature of 1000°C for 5 hours. The results of calcination was reacted with $(\text{NH}_4)_2\text{HPO}_4$, then dried at 110°C for 5 hours. Sintering was conducted to results of precipitated dried with temperature variations 400–1000°C for a hour each variation of temperature then characterized by X-ray diffractometer and FTIR in order to obtain the optimum formation temperature of hydroxyapatite is 800°C. The hydroxyapatite is then tested its effectiveness in protection against tooth demineralization using acetate buffer pH 5.0 with 1M acetic acid concentration with the addition of hydroxyapatite and time variation of immersion. The results showed that the rate of tooth demineralization in acetate buffer decreased significantly with the provision of hydroxyapatite into a solution where the addition of the magnitude of hydroxyapatite is greater decrease in the rate of tooth demineralization.

1. Introduction

Hydroxyapatite biomaterials are materials that are very widely used in several health purposes, including as a source of calcium for the manufacture of toothpaste and an important material in the formation/bone repair. The chemical properties of hydroxyapatite are bioactive and compatible with the adjacent bone and teeth. Hydroxyapatite is a calcium phosphate ceramic that is totally biocompatible and nontoxic and becomes an integral part of living bone and teeth tissue [1–8]. So it is important that these materials are produced independently. The raw material for the production of hydroxyapatite biomaterial is very easily available and abundant in Indonesia. The production process was easy and the cost is also relatively inexpensive if done on a large scale. Among the abundant raw materials are the shells of crabs, which are one of Indonesia's main export commodities. Export of Crabs commodity by Indonesia amounted to

604.215–625.000 tons/year without the shell form, while domestic consumption is expected to be so much more, as in Makassar, carrying 292.5 tons exported in the form of crab without shell with the main export destination being Singapore [9]. If the mass of crab shells 25–50% of the total mass, it can be estimated that in 2012 produced the shells of crabs around 151,053.75 to 302,107.5 tons in Indonesia and 73.125 to 146.25 tons in Makassar (a region of Indonesia), there was just from crabs production were exported. This value is of course even more if the crab's consumptions in the country are also taken into account. This suggests the existence of crab shells is abundant in Indonesia, including in Makassar. As known in Indonesia, the shells of crabs have not been used, so it will only be a waste disturbing environment [7, 8].

Crabs shells containing calcium carbonate (CaCO_3) are very abundant; amount 40–70%, varies according to the species [7]. Calcium carbonate can be further processed into

calcium hydroxyapatite [$\text{Ca}_{10}(\text{PO}_4)_6(\text{OH})_2$] [4, 5]. According to Strassler [10], hydroxyapatite is one of the active ingredient materials that are widely used in toothpaste products for protection against teeth demineralization [11–13].

The crystals structure of hydroxyapatite will be better by using CaO as a precursor of calcium. However, the use of these compounds also produces carbonate apatite [$\text{Ca}_{10}(\text{PO}_4)_6\text{CO}_3$] in a fairly large percentage. This is because the calcination process cannot completely eliminate carbon dioxide (CO_2) in CaCO_3 so that there can be reaction with the precursor phosphate. However, the carbonate apatite heating at a temperature of 700°C – 900°C for 2–5 hours, followed by washing using distilled water, the carbonate apatite can be hydroxyapatite [11–13]. The instrument were used in this research were glass apparatus, Ohaus analytical balance, petri dish, porcelain cup, Buchner flask, Buchner funnel, vacuum pump Sargent-Welch Co. Model 1400, magnetic stirrer, magnetic bar, hotplate Idealife, pH meter, Furnace Thermolyse 6000–Barnstead, dessicator, thermometers, Spnissosfd oven, stopwatch, Shimadzu X-ray diffractometer (XRD) Model 6000, X-ray Fluorescence (XRF) Shimadzu, Fourier Transform Infra-Red (FTIR) Prestige-21 Shimadzu, Scanning Electron Microscopy combined with the ability to generate localized chemical information (SEM-EDXA) Variant, and UV-VIS Shimadzu model 6105. This is because the carbonate ion compounds are able to inhibit the crystallization process $\text{Ca}_{10}(\text{PO}_4)_6(\text{OH})_2$ so that the results will be dominated by an amorphous phase [14].

The calcinations temperatures of CaCO_3 range from 900°C to 1200°C . If the CaCO_3 burned at temperature calcinations, decomposition reaction of CaCO_3 into CaO will occur and CO_2 emissions are dominant and will be issued as a result of the combustion reaction [13–15].

2. Experimental

2.1. Research Materials. The following materials used are as follows. Waste of crabs shells *Portunus pelagicus* species was taken from an exporter crabs company in industry areal, Makassar city, south Sulawesi province, Indonesia. Tooth samples were taken from Dr. Wahidin hospital, and $(\text{NH}_4)_2\text{HPO}_4$ was obtained from Fluka chemical, CH_3COOH glacial 100%, $\text{CH}_3\text{COONa}\cdot 3\text{H}_2\text{O}$ from Merck, $(\text{NH}_4)_6\text{Mo}_7\text{O}_{24}\cdot 4\text{H}_2\text{O}$ from Aldrich, NH_4VO_3 from Aldrich, HNO_3 and NaF from Fluka chem., $(\text{NH}_4)_2\text{C}_2\text{O}_4$, distilled water, aluminum foil, and Whatman filter paper numbers 40 and 42.

2.2. Research Instruments. The instruments were used in this research that glass as commonly used in laboratories, Ohaus analytical balance, petri dish, porcelain cup, Buchner flask, Buchner funnel, vacuum pump Sargent-Welch Co. Model 1400, magnetic stirrer, magnetic bar, hotplate Idealife, pH meter, Furnace Thermolyse 6000 Barnstead, dessicator, thermometers, oven Spnissosfd, stopwatch, Shimadzu X-ray diffractometer (XRD) Model 6000, X-ray fluorescence (XRF) Shimadzu, Fourier transform infrared (FTIR) Prestige-21 Shimadzu, scanning electron microscopy combined with the

ability to generate localized chemical information (SEM-EDXA) variant, and UV-VIS Shimadzu model 6105.

2.3. Synthesis of Hydroxyapatite from Waste Shell Crab *Portunus pelagicus*. Crabs shells *Portunus pelagicus* waste was cleaned with distilled water and dried at room temperature. Furthermore, to transform crabs shells into CaCO_3 and then in CaO, calcinations were performed on the samples at 1000°C temperature for 5 hours at a rate of temperature rise $5^\circ\text{C}/\text{minute}$. The containment of calcium (Ca) was determined by using XRF. Calcium oxide (CaO) obtained dominated as result of calcinations and then made suspensions in 100 mL of distilled water with a calcium concentration 0.3 M. The suspensions reacted by dropwise with a 100 mL 0.2 M of $(\text{NH}_4)_2\text{HPO}_4$ solution through the coprecipitation method, at temperatures around 40°C while the solution was stirred for 24 hours. The precipitation allowed stand overnight or 24 hours at room temperature, and the precipitate is filtered with a Whatman filter paper number 40 and dried at 110°C for 5 hours. The pure hydroxyapatite obtained by sintering the dried precipitate at various temperatures of 500°C – 900°C for 4 hours [16, 17]. The results washed with distilled water and then dried at a temperature of 110°C . The characterization of the compounds was performed by using X-ray diffraction (XRD), FTIR, and SEM-EDXA.

2.4. The Teeth Demineralization Tested. The proven in vitro demineralization of teeth was conducted through evaluating the concentration of phosphate in solution by using the UV-Vis spectroscopy. The effectiveness of hydroxyapatite protection against teeth demineralization was tested in acetate buffer pH 5.0 solutions, with 1 M of acetic acid concentration with the addition of hydroxyapatite in varying concentrations and immersion time [18]. Each of 5 beakers was filled with 300 mL of acetate buffer pH 5.0 with acetic acid concentration of 1 M. An acetate buffer was left without adding anything as a comparison. An acetate buffer was then added 10 ppm of NaF left without addition of $\text{Ca}_{10}(\text{PO}_4)_6(\text{OH})_2$. Other three pieces beaker of acetate buffer containing 10 ppm of NaF are adding of $\text{Ca}_{10}(\text{PO}_4)_6(\text{OH})_2$ with variation concentration of 25 ppm, 50 ppm, and 100 ppm. The cleaned tooth samples were immersed in each of 5 beakers of solutions. The immersed times of tooth samples in solution are 3, 6, 9, 24, and 48 hours, respectively. Furthermore, the phosphate concentration in each solution was measured by using UV-Vis spectrophotometer with the wavelength for phosphate (λ_{maks}) being 432 nm.

3. Results and Discussion

3.1. Calcinations of Crab Shells. Synthesis $\text{Ca}_{10}(\text{PO}_4)_6(\text{OH})_2$ begins with a calcinations crab shell at 1000°C for 5 hours. The calcinations aim to eliminate the organic component in the shells of crabs and convert CaCO_3 compound which is the dominant compound in the shells of crabs into CaO through the elimination of CO_2 in gas form. Characterizing the calcinations results was conducted by X-ray, XRF, and FTIR. The results can be seen from the diffraction pattern of the crab shells before and after calcinations at a temperature of

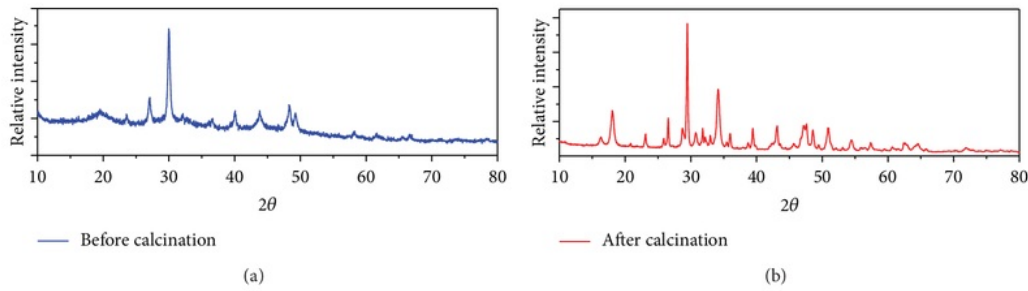


FIGURE 1: Diffractogram of crab shell; (a) before calcinations and (b) after calcinations at temperature 1000°C for 5 hours.

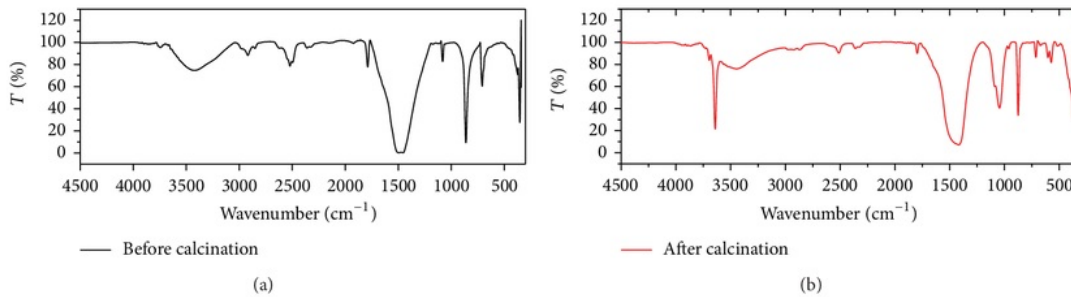


FIGURE 2: FTIR spectra of crab shells (a) before calcinations and (b) after calcinations at a temperature 1000°C for 5 hours.

1000°C for 5 hours (Figure 1). In this figure can be observed changes in the diffraction pattern of crab shells, where the change in the diffraction pattern is due to the chemical change from mixture of CaCO_3 with organic matter to pure CaO . The appearance of the sharper peaks in Figure 1 after calcinations (b) is a result of the crystallinity of the CaO .

Identification by FT-IR as shown in Figure 2 showed there is a reduction process of $-\text{CO}_3$ groups and some of IR-spectra were missing after calcinations. This shows the elimination of CO_2 and organic components occurred [19]. The elimination of $-\text{CO}_3$ groups and organic components can also be seen from the data of mass reduction of sample calcinations. Mass reduction during the calcinations process is 56.35% on average. This means that the efficiency of calcium compounds produced by 43.64%.

The determinations of calcium contained in sample was conducted by using X-ray fluorescence, where obtained calcium is 66.62% after calcinations. These results are then used to calculate the stoichiometry in determining the number of results calcinations which is needed to react with $(\text{NH}_4)_2\text{HPO}_4$ as the precursor phosphate.

3.2. Precipitation with Phosphate Precursors. The precipitation reactions aiming to produce $\text{Ca}_{10}(\text{PO}_4)_6(\text{OH})_2$ used phosphate, $(\text{NH}_4)_2\text{HPO}_4$, as the precursor and then reacted with CaO as calcinations results. Side results $\text{Ca}_{10}(\text{PO}_4)_6\text{CO}_3$ also occur as a product of reaction of $(\text{NH}_4)_2\text{HPO}_4$ and CaCO_3 presence in the calcinations results.

Dried precipitate further sintered on temperature variations of 400°–1000°C for 2 hours; it is intended to determine

the optimum temperature where the $\text{Ca}_{10}(\text{PO}_4)_6(\text{OH})_2$ is formed, furthermore characterized by using XRD, FT-IR, and SEM-EDXA.

3.3. Characterization of Sintering Results by XRD. XRD Diffractograms of compounds results presented in Figure 3. The diffractograms of each sintering results compounds indicate that the temperature is closely related to the formation of crystals. This is due to the nature of the vibrating atoms moving faster in higher temperatures [19].

The optimum temperature formation of hydroxyapatite was determined by calculation of the probability of the sample phase from the XRD results analysis according to JCPDS standard data, which, JCPDS; 24-0033 is standard data for $\text{Ca}_{10}(\text{PO}_4)_6(\text{OH})_2$; 09-0169 for $\beta\text{-Ca}_3(\text{PO}_4)_2$; 29-0359 for $\alpha\text{-Ca}_3(\text{PO}_4)_2$, 35-0180 $\alpha\text{-Ca}_3(\text{PO}_4)_2$; 35-0180 for $\text{Ca}_{10}(\text{PO}_4)_6\text{CO}_3(\text{OH})_2$ and 19-0272 standard data for $\text{Ca}_{10}(\text{PO}_4)_6\text{CO}_3(\text{OH})_2$. Figures 3 and 4 showed that the temperature is closely associated with the formation of hydroxyapatite phase. In the both graphs it can be seen that the maximum intensity of the phase formation of hydroxyapatite **has** been found by sintering at temperature of 800°C, it means the optimum temperature of hydroxyapatite formation **is** 800°C, and **then** this result will be used for another application.

The formations of hydroxyapatite phase had been dominated at 800°C confirmed by percentage probability sample phase (Figure 5), in which the percentage of hydroxyapatite phase formed around 46.61%, while phases of $\alpha\text{-Ca}_3(\text{PO}_4)_2$ and phase $\beta\text{-Ca}_3(\text{PO}_4)_2$ are 17.76% and 19.37%,

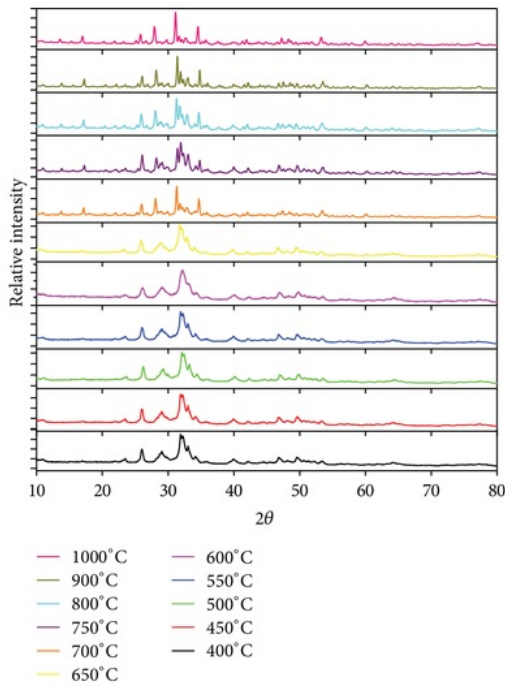


FIGURE 3: Diffraction patterns as a function of temperature sintering of hydroxyapatite.

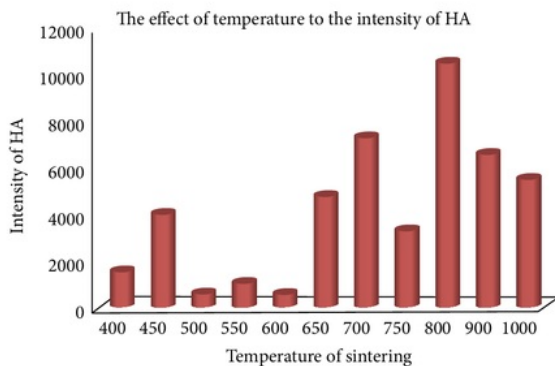


FIGURE 4: The influence of sintering temperatures on the formation of hydroxyapatite phase.

respectively. However, also there is still presence of a phase $\text{Ca}_{10}(\text{PO}_4)_6\text{CO}_3$ and $\text{Ca}_{10}(\text{PO}_4)_6\text{CO}_3(\text{OH})_2$ with a range of 11.84% and 4.43%, respectively, which indicates the presence of carbonates. All data coming from the calculations of the XRD spectrum used its software.

The X-ray diffractograms of $\text{Ca}_{10}(\text{PO}_4)_6(\text{OH})_2$ synthesized at a 800°C temperature sintering can be seen in Figure 6, where the peaks of HA are symbolized by the peak of the crystal $\text{Ca}_{10}(\text{PO}_4)_6(\text{OH})_2$, while peak α -TKF is symbolized crystalline peaks of $\alpha\text{-Ca}_3(\text{PO}_4)_2$, the symbol β -TKF for crystalline $\beta\text{-Ca}_3(\text{PO}_4)_2$, AKA for $\text{Ca}_{10}(\text{PO}_4)_6\text{CO}_3$,

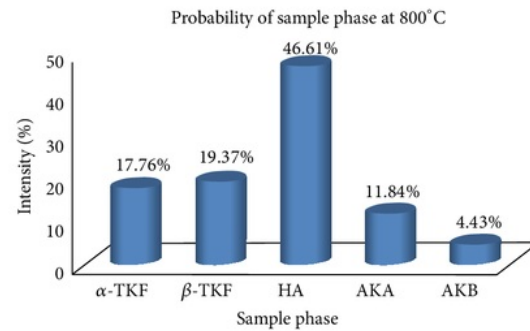


FIGURE 5: Percentage probability sample phase sintering at a temperature 800°C , where HA = $\text{Ca}_{10}(\text{PO}_4)_6(\text{OH})_2$, α -TKF = $\alpha\text{-Ca}_3(\text{PO}_4)_2$, β -TKF = $\beta\text{-Ca}_3(\text{PO}_4)_2$, AKA = $\text{Ca}_{10}(\text{PO}_4)_6\text{CO}_3$ and AKB = $\text{Ca}_{10}(\text{PO}_4)_6\text{CO}_3(\text{OH})_2$.

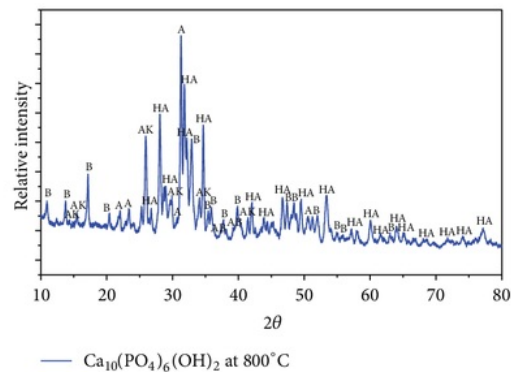


FIGURE 6: Diffractogram of sample were sintered at 800°C , where, HA = $\text{Ca}_{10}(\text{PO}_4)_6(\text{OH})_2$, A = $\alpha\text{-TKF} = \alpha\text{-Ca}_3(\text{PO}_4)_2$, B = $\beta\text{-TKF} = \beta\text{-Ca}_3(\text{PO}_4)_2$, AK = AKA = $\text{Ca}_{10}(\text{PO}_4)_6\text{CO}_3$ and AB = AKB = $\text{Ca}_{10}(\text{PO}_4)_6\text{CO}_3(\text{OH})_2$.

and AKB for $\text{Ca}_{10}(\text{PO}_4)_6\text{CO}_3(\text{OH})_2$. The highest intensity peak at 31.2572° corresponding to crystalline $\alpha\text{-Ca}_3(\text{PO}_4)_2$ is seen, the second highest peak intensity is 31.7783° , and the third highest peak intensity is 28.0565° crystals suitable for $\text{Ca}_{10}(\text{PO}_4)_6(\text{OH})_2$.

3.4. Characterization of Ca-Hydroxyapatite with FT-IR. FTIR results showed that the sintering temperature variation affects the absorption band shapes which generally all sintering results showed absorption band of $-\text{OH}$, absorption band ν_1 , ν_2 , ν_3 , and ν_4 of PO_4^{3-} , and CO_3^{2-} groups. Infrared spectra in Figure 7 show the $-\text{OH}$ groups at 633 cm^{-1} which are characteristic of hydroxyapatite [17] appearing on the sintering temperatures of $400\text{--}1000^\circ\text{C}$. Additionally spectrum also showed higher sintering temperature causing the sharper peaks phosphate group (PO_4^{3-}) because the nature of the vibrating atoms moves faster at higher temperatures [19]. The presence of the phosphate group indicates the formation of hydroxyapatite in the precipitates.

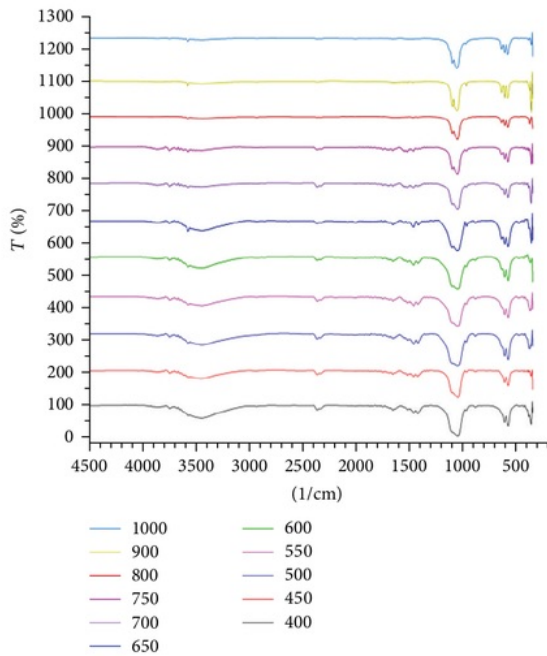


FIGURE 7: FT-IR spectra of synthesis results in various temperatures (400–1000°C).

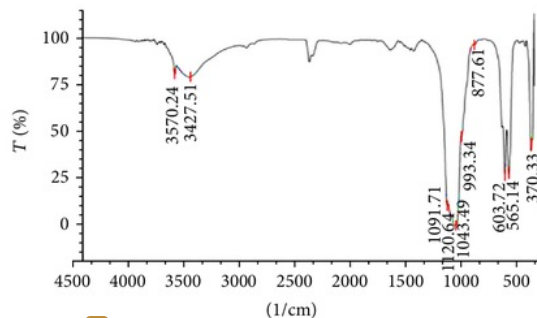
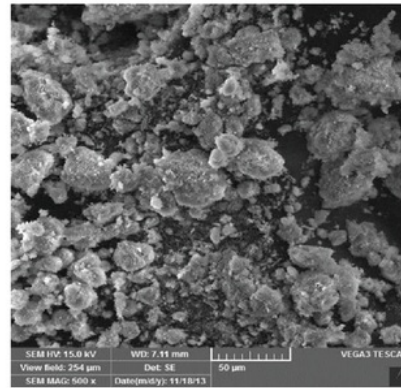
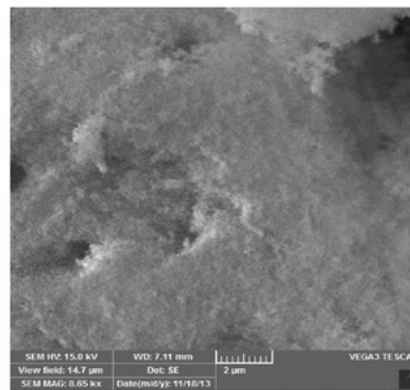


FIGURE 8: FT-IR spectra of hydroxyapatite (HA) were sintered at 800°C.

The FT-IR spectra of sample were sintered at a temperature of 800°C (Figure 8) showing that hydroxyapatite is the dominant compound formed. The stretching frequencies of PO_4 group are indicated by 1120.64 cm^{-1} , 1091.71 cm^{-1} , 1043.49 cm^{-1} (ν_3), 993.34 cm^{-1} , 877.61 cm^{-1} (ν_1), 603.72 cm^{-1} , 565.14 cm^{-1} (ν_4), and 370.33 cm^{-1} (ν_2). And a sharp spectrum in the area of 3570.24 cm^{-1} indicates the presence of free $-\text{OH}$ and 3427.51 cm^{-1} indicating $-\text{OH}$ bounded, and this is indicating that the dominant compound is $\text{Ca}_{10}(\text{PO}_4)_6(\text{OH})_2$. While area of 1654.92 cm^{-1} , 1458.18 cm^{-1} , and 1421.54 cm^{-1} indicates the presence of carbonate groups (CO_3^{2-}) it can be identified as $\text{Ca}_{10}(\text{PO}_4)_6\text{CO}_3$



(a)



(b)

FIGURE 9: The SEM graph of hydroxyapatite (HA) synthesis from crab shells.

and $\text{Ca}_{10}(\text{PO}_4)_6\text{CO}_3(\text{OH})_2$ which has not been transformed into $\text{Ca}_{10}(\text{PO}_4)_6(\text{OH})_2$ during the sintering process.

3.5. Characterization of Ca-Hydroxyapatite Sintered at 800°C with SEM-EDXA. The results of characterization by SEM-EDXA shown in Figure 9(a) show that the size of hydroxyapatite formed from the synthesis tends to be small and only a few are large. While Figure 9(b) shows that the surface of hydroxyapatite is smooth and nonporous, this shows that hydroxyapatite which has synthesis from crab shells can function well as inhibiting tooth demineralization [13].

While in Figure 10 the EDXA spectrum shows the composition of the synthesis yield was dominated by oxygen (O) up to 59.52%, calcium (Ca) up to 23.76%, and phosphorus (P) up to 13.32%. The composition confirmed the composition of hydroxyapatite. It can be concluded that the synthesis results can be achieved to target.

3.6. Inhibition of Tooth: The Demineralization by Presence of $\text{Ca}_{10}(\text{PO}_4)_6(\text{OH})_2$. Demineralization of teeth is a process of decomposition of the crystal of $\text{Ca}_{10}(\text{PO}_4)_6(\text{OH})_2$ due

TABLE 1: Percentage teeth mass remaining on immersion in acetate buffer solution with a certain variation of the treatment for 48 hours.

Number	Code sample	Initial mass (gram)	Final mass (gram)	Percentage (%)	
1	TP	G 1	1,54	1,52	98,21
		G 2	1,07	1,04	97,81
		G 3	1,73	1,69	97,55
		Total			97,86
2	P	G 1	0,79	0,77	96,96
		G 2	0,82	0,79	96,85
		G 3	1,17	1,15	97,99
		Total			97,27
3	25	G 1	1,97	1,92	97,74
		G 2	1,23	1,21	98,84
		G 3	1,65	1,62	97,81
		Total			98,13
4	50	G 1	0,91	0,89	98,33
		G 2	1,20	1,18	98,01
		G 3	1,26	1,24	98,10
		Total			98,15
5	100	G 1	1,4589	1,44	98,70
		G 2	1,053	1,0307	97,88
		G 3	1,4709	1,4448	98,22
		Total			98,27

G = teeth.

TP = acetate buffer without the addition of any NaF and $\text{Ca}_{10}(\text{PO}_4)_6(\text{OH})_2$.

P = acetate buffer with only the addition of NaF.

25 = acetate buffer addition of NaF and 25 ppm of $\text{Ca}_{10}(\text{PO}_4)_6(\text{OH})_2$.

50 = acetate buffer addition of NaF and 50 ppm of $\text{Ca}_{10}(\text{PO}_4)_6(\text{OH})_2$.

100 = acetate buffer addition of NaF and 100 ppm of $\text{Ca}_{10}(\text{PO}_4)_6(\text{OH})_2$.

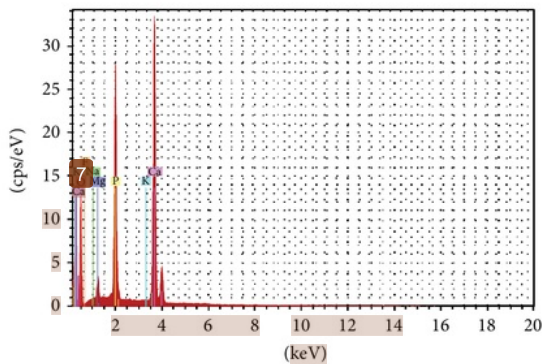


FIGURE 10: The EDXA spectrum of hydroxyapatite (HA) synthesis from crab shells.

to the acidic conditions by releasing Ca^{2+} and PO_4^{3-} ions. Demineralization of tooth causing increased levels of Ca^{2+} and PO_4^{3-} in saliva in direct contact with the tooth. In vitro, the rate of tooth demineralization can be observed through the concentrations of Ca^{2+} and PO_4^{3-} ions in solutions where the tooth was soaked each unit of time. Therefore, increase of PO_4^{3-} ions concentrations in solution a soaked

gear can be one of indicators to measure the rate of tooth demineralization.

Figure 11 shows the relationship between the soaking time of teeth versus the increase of the ion PO_4^{3-} levels in solution where the tooth was soaked as well; it appears that with the increasing addition of $\text{Ca}_{10}(\text{PO}_4)_6(\text{OH})_2$ into the acetate buffer equals to the rate of demineralization decrease. It can be altered by the amount of PO_4^{3-} ions in solutions; however the addition of $\text{Ca}_{10}(\text{PO}_4)_6(\text{OH})_2$ ions showed lower amount of PO_4^{3-} ions compared to solutions without the addition of $\text{Ca}_{10}(\text{PO}_4)_6(\text{OH})_2$. This proves that the $\text{Ca}_{10}(\text{PO}_4)_6(\text{OH})_2$ were synthesized from the crab shell effective for protection against tooth demineralization.

The decrease in the rate of tooth demineralization with the addition of $\text{Ca}_{10}(\text{PO}_4)_6(\text{OH})_2$ can also be observed through analyzing the tooth mass reduction in the fifth variation of acetate buffer solution as shown in Table 1. The greater concentrations of $\text{Ca}_{10}(\text{PO}_4)_6(\text{OH})_2$ in the acetate buffer solution were teeth immersed exhibit the smaller mass of teeth in the solution [19].

Table 1 shows the relationship between tooth mass and the addition of hydroxyapatite.

4. Conclusion

Based on these results it is concluded as follows.

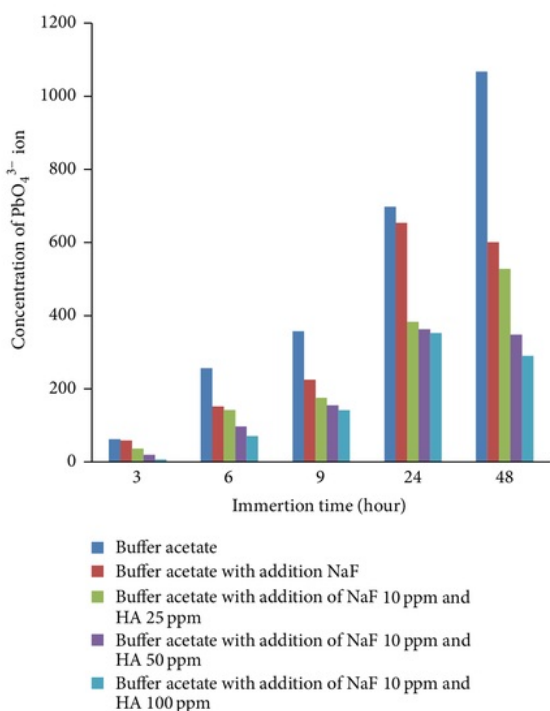


FIGURE 11: Relationship between teeth immersion time versus PO_4^{3-} ion concentration in a solution where teeth soaked or immersed.

- (1) Waste of shells crabs (*Portunus pelagicus*) proved to be used as raw material for the synthesis of $Ca_{10}(PO_4)_6(OH)_2$ due to high calcium levels which amounted to 66.62% in addition to the abundant existence as waste.
- (2) The optimum temperature formation of $Ca_{10}(PO_4)_6(OH)_2$ is at $800^\circ C$.
- (3) $Ca_{10}(PO_4)_6(OH)_2$ were synthesized from waste of shell crabs (*Portunus pelagicus*) in vitro effectively inhibiting the rate of demineralization of the tooth where the greater the addition of $Ca_{10}(PO_4)_6(OH)_2$ in the solution, the more the inhibiting demineralization of the tooth or the smaller the rate of tooth demineralization in solution.

Conflict of Interests

The authors declare that there is no conflict of interests regarding the publication of this paper.

Acknowledgments

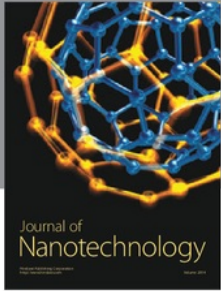
The authors gratefully acknowledge the Director General of Higher Education that has funded this research through a MP3EI grant in 2013 and 2014. Thanks are also conveyed to Dr. Dahlang (Department of Physics, FMIPA-UNHAS) which has measured XRF and XRD. Similarly the authors

thank the UNM Materials Physics Laboratory that has measured XRD and SEM-EDXA and also pronounced thanks to Dr. Kartini (Integrated Chemistry Laboratory UNHAS) who has helped measurement of FTIR and UV-Vis.

References

- [1] J. S. Wefel and M. W. J. Dodds, *Oral Biologic and the Demineralization and Remineralization of Teeth*, Appleton & Lange, Stamford, Conn, USA, 1999.
- [2] M. Jarcho, "Biomaterial aspects of calcium phosphates. Properties and applications," *Dental Clinics of North America*, vol. 30, no. 1, pp. 25–47, 1986.
- [3] G. L. de Lange, C. de Putter, and F. L. J. de Wijs, "Histological and ultrastructural appearance of the hydroxyapatite-bone interface," *Journal of Biomedical Materials Research*, vol. 24, no. 7, pp. 829–845, 1990.
- [4] B. M. Tracy and R. H. Doremus, "Direct electron microscopy studies of the bone-hydroxylapatite interface," *Journal of Biomedical Materials Research*, vol. 18, no. 7, pp. 719–726, 1984.
- [5] D. E. Steflink, R. V. McKinney Jr., and D. L. Koth, "Epithelial attachment to ceramic dental implants," *Annals of the New York Academy of Sciences*, vol. 523, pp. 4–18, 1988.
- [6] K. Donath and G. A. Breuner, "A method for the study of undecalcified bones and teeth with attached soft tissues. The Säge-Schliff (sawing and grinding) technique," *Journal of Oral Pathology*, vol. 11, no. 4, pp. 318–326, 1982.
- [7] P.-I. Brånemark, G. A. Zarb, and T. Albrektsson, *Tissue-Integrated Prostheses: Osseointegration in Clinical Dentistry*, Quintessence Publishing, Chicago, Ill, USA, 1985.
- [8] L. Linder, "High-resolution microscopy of the implant-tissue interface," *Acta Orthopaedica Scandinavica*, vol. 56, no. 3, pp. 269–272, 1985.
- [9] BPS, *Data Hasil Ekspor Kepiting pada Tahun 2011*, BPS, 2012, <http://sulsel.bps.go.id/archives/49867>.
- [10] Harianingsih, *Pemanfaatan limbah cangkang kepiting menjadi kitosan sebagai Bahan Pelapis (Coater) pada Buah Stroberi [M.S. thesis]*, Diponegoro University, Semarang, Indonesia, 2010.
- [11] S. U. Dewi, *Pembuatan Komposit Kalsium Fosfat-Kitosan dengan Metode Sonikasi [thesis]*, Post Graduate Program of Bogor Agricultural University, Bogor, Indonesia, 2009.
- [12] H. E. Strassler, *Toothpaste Ingredients*, 2011, http://d3e9u3gw8odyw8.cloudfront.net/toothpaste_ingredients.pdf.
- [13] E. Fujii, K. Kawabata, Y. Nakazaki et al., "Fabrication of hydroxyapatite with controlled morphology in a micro-reactor," *Journal of the Ceramic Society of Japan*, vol. 119, no. 1386, pp. 116–119, 2011.
- [14] S. Ramkumar, W. Wang, S. Li et al., "Carbonation—Calcination Reactions (CCR) Process for High Temperature CO_2 and Sulfur Removal," 2011, <http://www.rsc.org/suppdata/jm/b9/b925776d/b925776d.pdf>.
- [15] F. Zulti, *Spektroskopi Inframerah, Serapan Atomik, Serapan Sinar Tampak dan Ultraviolet Hidroksiapatit dari Cangkang telur [Ph.D. thesis]*, Department of Physics, Faculty of Mathematics and Natural Sciences, Institute of Agriculture Bogor, Bogor, Indonesia, 2008.
- [16] R. Samsiah, *Karakterisasi Biokomposit Apatit-Kitosan dengan XRD (X-Ray Diffraction), FTIR (Fourier Transform Infrared), SEM (Scanning Electron Microscopy) dan Uji Mekanik [M.S. thesis]*, Department of Physics, Faculty of Mathematics and Natural Sciences, Institute of Agriculture Bogor, Bogor, Indonesia, 2009.

- [17] E. C. Reynolds, "Anticariogenic of amorphous calcium phosphate complexes stabilized by casein phosphopeptide," *U.S. Dentistry*, vol. 8, pp. 51-54, 1998.
- [18] R. L. Karlinsey, A. C. Mackey, T. J. Walker et al., "In vitro remineralization of human and bovine white-spot enamel lesions by NaF dentifrices: a pilot study," *Journal of Dentistry and Oral Hygiene*, vol. 3, no. 2, pp. 22-29, 2011.
- [19] *JOMI on CD-ROM, 1993 Jan (69-74): Bone Reactions to Hydroxyapatite-Coated Dental*, Quinte, 1993.



Journal of
Nanotechnology



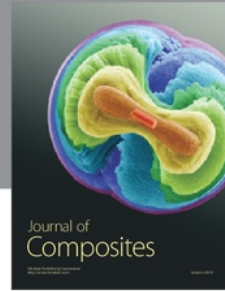
International Journal of
Corrosion



International Journal of
Polymer Science



Smart Materials
Research



Journal of
Composites

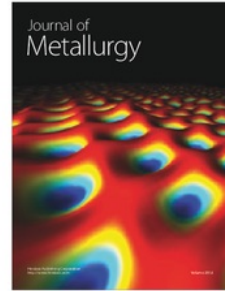


BioMed
Research International



Hindawi

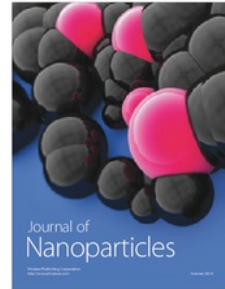
Submit your manuscripts at
<http://www.hindawi.com>



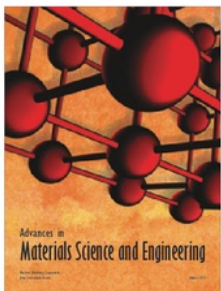
Journal of
Metallurgy



Journal of
Materials



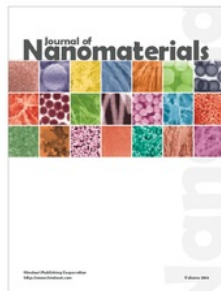
Journal of
Nanoparticles



Advances in
Materials Science and Engineering



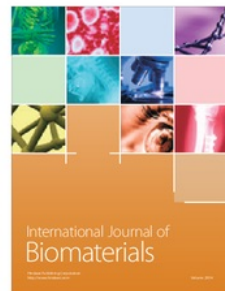
Scientifica



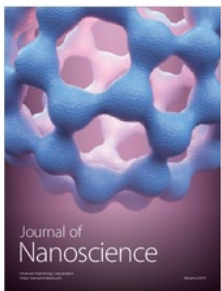
Journal of
Nanomaterials



The Scientific
World Journal



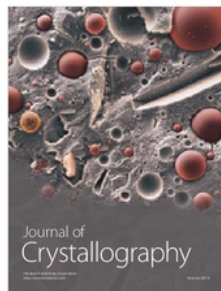
International Journal of
Biomaterials



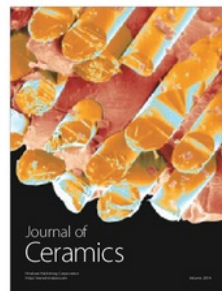
Journal of
Nanoscience



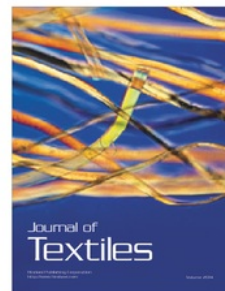
Journal of
Coatings



Journal of
Crystallography



Journal of
Ceramics



Journal of
Textiles

Synthesis and Characterizations of Calcium Hydroxyapatite Derived from Crabs Shells (*Portunus pelagicus*) and Its Potency in Safeguard against to Dental Demineralizations

ORIGINALITY REPORT

% **8**

SIMILARITY INDEX

% **3**

INTERNET SOURCES

% **3**

PUBLICATIONS

% **4**

STUDENT PAPERS

PRIMARY SOURCES

1

linknovate.com

Internet Source

% **1**

2

Submitted to Curtin University of Technology

Student Paper

% **1**

3

Submitted to Institute of Research & Postgraduate Studies, Universiti Kuala Lumpur

Student Paper

% **1**

4

ns2.quintpub.com

Internet Source

% **1**

5

Is Fatimah, Greef Rose Aulia, Wellyana Puspitasari, Rico Nurillahi, Lusi Sophia, Rivaldo Herianto. "Microwave-synthesized hydroxyapatite from paddy field snail (*Pila ampullacea*) shell for adsorption of bichromate ion", Sustainable Environment Research, 2018

Publication

<% **1**

6

Teng, X.G.. "Study on thermal decomposition of lithium hexafluorophosphate by TG-FT-IR

<% **1**

coupling method", *Thermochimica Acta*,
20051001

Publication

7

ir.uiowa.edu

Internet Source

<% 1

8

Miculescu Florin, Mocanu A. Cătălina, Stan E. George, Maidaniuc Andreea, Miculescu Marian, Voicu S. Ioan, Iulian Antoniac. "Bioceramics Derived from Marble and Sea Shells as Potential Bone Substitution Materials", Wiley, 2019

Publication

<% 1

9

Hidekazu Tanaka, Akemi Yasukawa, Kazuhiko Kandori, Tatsuo Ishikawa. "Surface structure and properties of fluoridated calcium hydroxyapatite", *Colloids and Surfaces A: Physicochemical and Engineering Aspects*, 2002

Publication

<% 1

10

D S Handayani, T Kusumaningsih, L A Hak. "Utilization Chitosan- Butylcalix[4]Arene for Red MX 8B Adsorbent ", *IOP Conference Series: Materials Science and Engineering*, 2017

Publication

<% 1

11

Submitted to iGroup

Student Paper

<% 1

Submitted to Wright State University

12

Student Paper

<% 1

13

Fu, R.. "A new sodium zinc 1,4-butylenediphosphonate with polar pillar-like open-framework", *Inorganic Chemistry Communications*, 200510

Publication

<% 1

14

"Abstracts", *Journal of Dental Research*, 2016

Publication

<% 1

15

core.ac.uk

Internet Source

<% 1

16

Submitted to Jawaharlal Nehru Technological University Anantapur

Student Paper

<% 1

17

Galang B. Raka Pambudi, Ita Ulfin, Harmami Harmami, Suprpto Suprpto, Fredy Kurniawan, Yatim L. Ni'mah. "Synthesis of water-soluble chitosan from crab shells (*Scylla serrata*) waste", *AIP Publishing*, 2018

Publication

<% 1

18

Jordanka Petrova. "SYNTHESIS AND STRUCTURE OF IRON(III) AND CHROMIUM(III) COMPLEXES OF 2-DIETHOXYPHOSPHONYL-2-PHENYLETHEN-1-OL", *Journal of Coordination Chemistry*, 9/1/1994

<% 1

EXCLUDE QUOTES ON

EXCLUDE
BIBLIOGRAPHY ON

EXCLUDE MATCHES < 5
WORDS